THE IFS of SPHERE: Integration and Laboratory Performances

R. Claudi[a], U. Anselmi[a], P. Bruno[b] , E. Cascone[c], A. Costille[d], V. De Caprio[c], S. Desidera[a], E. Giro[a], R. Gratton[a], L. Lessio[a], D. Mesa[a], S. Scuderi[b], M. Turatto[a], F.Wildi[e], A. Baruffolo[a] , R. Dorn[f] , D. Fantinel[a], G. Finger[f], J.L. Lizon[f], E. Sant'Ambrogio[d], B. Salasnich[a], Jl. Beuzit[d], K. Dohlen[f] , P. Puget[d], M. Kasper[f], N. Hubin[f]

[a] INAF, Osservatorio Astronomico di Padova, Vicolo dell'Osservatorio 5, 35122 Padova, Italy
[b] INAF, Osservatorio Astrofisico di Catania, Italy INAF-IASF, via E. Bassini 15, 20133 Milano, Italy
[c] INAF, Osservatorio Astronomico di Capodimonte, Salita Moiariello 16, 80131 Napoli, Italy
[d] UJF-Grenoble, CNRS/INSU Institute de Planetologie' et d'Astrophysique de Grenoble (IPAG), UMR 5274, 38041 Grenoble, France
[e] Observatoire de Geneve', 51 ch des Maillettes, CH-1290 Sauverny, Switzerland
[f] European Southern Observatory Germany
[g] Laboratoire d'Astrophysique de Marseille, B.P. 8, F-13376 Marseille Cedex 12, France

ABSTRACT

SPHERE is an exo-solar planet imager, which goal is to detect giant exo-solar planets in the vicinity of bright stars and to characterize them through spectroscopic and polarimetric observations. It is a complete system with a core made of an extreme-Adaptive Optics (AO) turbulence correction, pupil tracker and NIR and Visible coronagraph devices. At its back end, a differential dual imaging camera and an integral field spectrograph (IFS) work in the Near Infrared (NIR) Y, J, H and Ks bands ($0.95 \leq \lambda \leq 2.32$ μm) and a high resolution polarization camera covers the visible ($0.6 \leq \lambda \leq 0.9$ μm). The IFS is a low resolution spectrograph (R~50) which works in the near IR ($0.95 \leq \lambda \leq 1.6$ μm), an ideal wavelength range for the detection of planetary features. The IFS is based on a new conception microlens array (BIGRE) of 145X145 lenslets designed to reduce as low as possible the contrast. The IFU will cover a field of view of about 1.7 x 1.7 square arcsecs reaching a contrast of 10^{-7}, giving an high contrast and high spatial resolution "imager" able to search for planet well inside the star PSF. In the last year it has been integrated onto the huge optical bench of SPHERE and fully tested.

Keywords: Exoplanets, Integral Field Spectroscopy

1. INTRODUCTION

SPHERE (Spectro-Polarimetric High-contrast Exoplanets Research) is a second generation instrument for VLT[1] optimized for high contrast imaging at the Nasmyth focus of one of the VLT units. SPHERE is made of four subsystems: the Common Path Optics and three science channels, a differential imaging camera (IRDIS), an Integral Field Spectrograph (IFS)[2], and a visible imaging polarimeter (ZIMPOL). The Common Path includes pupil stabilizing foreoptics (tip-tilt and derotator) where insertable polarimetric half-wave plates are also provided, the SAXO extreme adaptive optics system with a visible wavefront sensor, and NIR coronagraphic devices in order to feed IRDIS and IFS with a highly stable coronagraphic image in the NIR. IFS explores the stellar neighborhood in order to find planetary spectral features. For the IFS, this quest is conducted searching for strong CH_4 absorption bands in both the stellar light reflected by gaseous Jupiter-like planets and in thermal emission from young-warm planets. Moreover it will be possible to have a first order characterization of the low mass companion itself. Additional science topics, which will be addressed by SPHERE, included the study of brown dwarfs, circumstellar disks and related phenomena such as mass loss.
The heart of IFS (see Figure 1) is a new kind of lens-based IFU called BIGRE[3] that is depicted in the inset of Figure 1. Specifically, BIGRE is placed at the interface of the instrument with the SPHERE Common Path (CP) and it is optically conjugated with the telescope Focal Plane, this latter being re-imaged by an F/# = 316

Ground-based and Airborne Instrumentation for Astronomy IV, edited by Ian S. McLean, Suzanne K. Ramsay, Hideki Takami, Proc. of SPIE Vol. 8446, 84468N · © 2012 SPIE · CCC code: 0277-786X/12/$18 · doi: 10.1117/12.924966

beam. This allows to sample the diffractive PSF - arising from the AO compensation and the Coronagraphic spatial filtering, working both inside the CP optics - at the Nyquist's limit. The purpose of this instrument is thus to realize diffraction limited Integral Field Spectroscopy with the high contrast capabilities of the BIGRE device as IFU. To this scope, the whole IFS system, which is downstream the entrance slits array should only re-image and disperse these slits with the highest optical stability and a good optical quality. To achieve this goal, the optimized IFS optical design is a fully dioptric concept design, shaped by several optics located along a straight optical axis. IFS is projected to work, with different resolution in two different wavelength ranges: with a resolution of R~50 in the 0.95 -1.35 μm (z-J mode) while a lower resolution (R~30) is considered for the wider wavelength range of 0.95 – 1.65 μm (z-J-H mode). The two different resolutions are achieved by two different Amici prisms. The two working wavelength ranges are defined by a combination of band pass, high pass and low pass filter mounted in two locations: inside the dewar (low pass filter) and just in front of prisms (band pass filter for the z-J mode and high pass filter for the z-J-H mode).

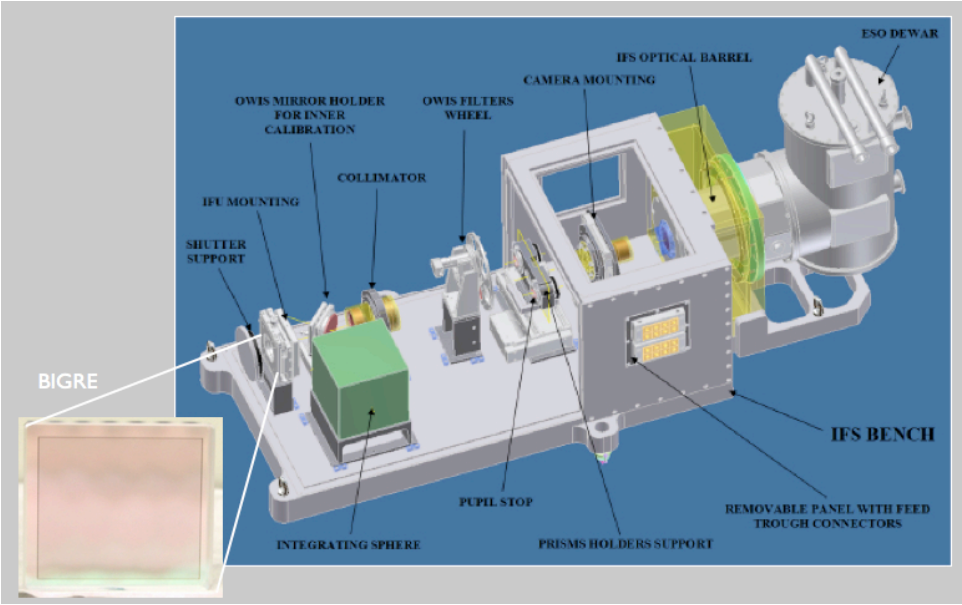

Figure 1: The SPHERE IFS Layout. In the inset the BIGRE and its location are shown

2. SPHERE IFS TESTS

The whole IFS underwent both functional and performance tests. The test strategy adopted was at first to perform all possible tests with stand alone IFS into the laboratory of the Astronomical Observatory of Padova. Further, once it has been integrated on the huge optical bench of SPHERE all tests were re-performed. In the next paragraphs a description is given of main stand-alone performance tests.

2.1 IFS Geometry

The purpose of this section is to describe the results of tests on the geometry of the spectra provided by the SPHERE IFS made at INAF-OAPD. The tests verify that the two IFS observing modes (z-J and z-J-H) for integral field spectroscopy in the near infrared are actually available and that the spectral range is [0.95-1.65] μm with a spectral sampling >30 per pixel. All these characteristics converge into the definition of the field of view of 1.35 x 1.35 [arcsec²] (goal 3 x 3 [arcsec²]). The latter specification can actually be verified only on sky, but in the laboratory we verified that the lenslet pitch is 161.5 μm (as measured by the vendor) and that the number of lenslets is large enough to cover the whole field of view at this sampling. Given the definition of the optical interface between Common Path and IFS (F/316.4), the lenslet pitch corresponds to the correct

sampling on sky of 12.25 mas. In order to perform the tests to verify the spectral properties of the IFS we have to illuminate the instrument with the white lamp provided by the Common Path Simulator (CPS), as well as with a number of monochromatic sources (lasers), in the two observing modes (Y-J and Y-H). The lasers had wavelength of 980, 1060, 1300, and 1550 nm. For all lamps and in all modes, a datacube of 50 images with 1 second DIT in Double Correlated Mode were obtained. A median of each image is obtained, and dark was subtracted. The images were then analyzed with specific IDL routines.

The IFS camera may move in both x and y direction by means of piezo motors. This allows to realize dithering of the images on the detector, which is very useful to achieve high S/N flat fielding (S/N>1000), and to reduce the impact of hot pixels and cosmic rays on final data.

Two dithering modes are foreseen for IFS (4x4 and 10x10). In both cases, images on the detector are shifted by 1 pixel for each step; the cycle is in closed raster mode. Dithering was tested by acquiring images obtained by illuminating the CPS with both laser and a continuum lamp in order to determine every dithering effects on wavelength calibration. Figure 2 shows portions of two images obtained with IFS in Y-H mode.

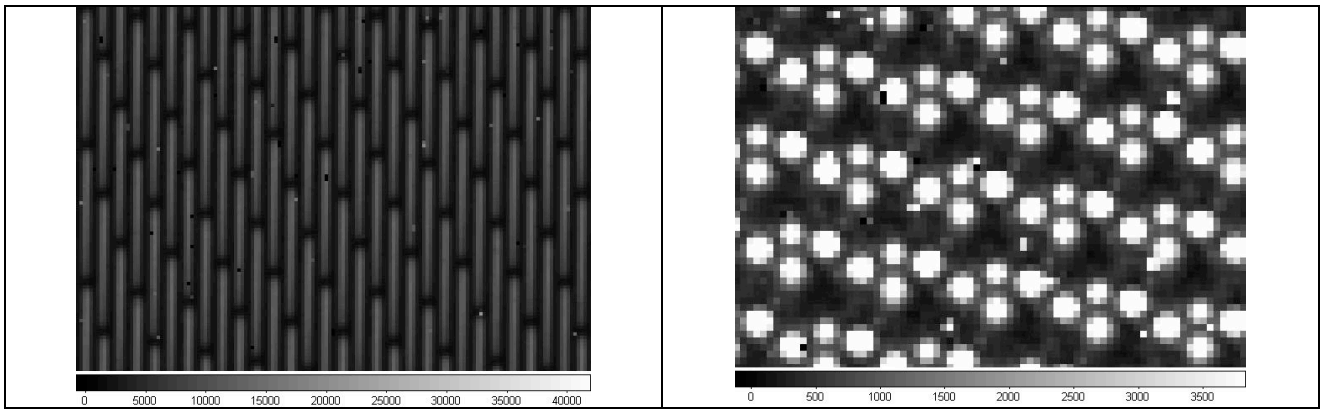

Figure 2. Right: portion of an image obtained with a white lamp with IFS in the Y-H mode; Portion of the sum of four different images obtained feeding the CP simulator with laser lamps (980, 1060, 1300 and 1550 nm) with IFS in the Y-H mode

In each image there are 23140 spectra. This corresponds to an area of 523 mm^2 on the BIGRE. This is 0.915 times the useful area of BIGRE. The rest falls outside the detector area. We measured directly on the images the separation between spectra, the spectral spacing and the length of each spectrum.

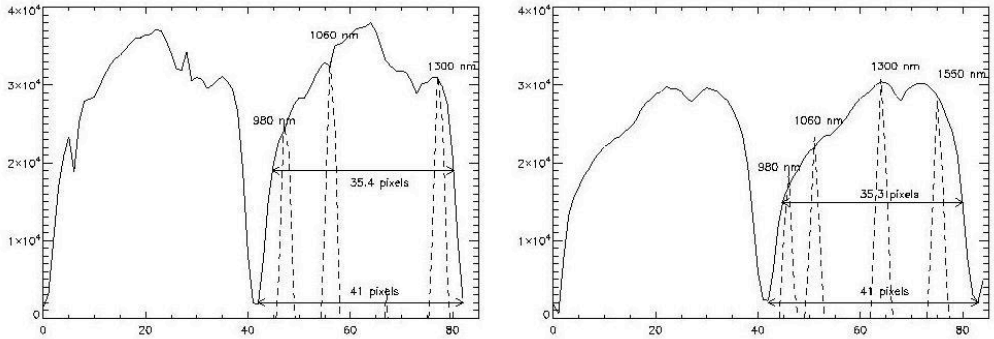

Figure 3. Plot of a small section of a detector row showing two consecutive white lamp spectra obtained with both IFS Y-J mode (left) and IFS Y-H Mode (right). Overimposed (dashed line) are the laser lamp spectra;

The wavelength range is obtained by means a linear fit of the dispersion relation while the spectral sampling ΔS is evaluated by the following:

$$\Delta S = \frac{\lambda_{cen}}{\lambda_{\max} - \lambda_{\min}} l$$

where: λ_{cen}, λ_{min} e λ_{max} are respectively the central, the minimum and the maximum wavelength of each spectrum and l the relative length of each spectrum. Figure 3 illustrates the geometry of the spectra for the Y-J and Y-H modes.
Table 1 gives a comparison between data about the measured geometry of the IFS and the expected values taken from the design of the instrument (Technical Specification).

Table 1. IFS Geometry

	Expected Value	Measured Value
Separation between spectra	4.96 pixels	5.093 pixels
Spectral spacing	40.12 pixels	41.0 pixels
Spectral length		
- Prism 1 (Y-J)	34.78 pixels	35.4 pixels (1)
- Prism 2 (Y-H)	34.0 pixels	35.3 pixels (1)
Wavelength Range		
- Prism 1 (Y-J)	0.95-1.35 μm	0.96-1.34 μm (1)
- Prism 2 (Y-H)	0.95-1.65 μm (TS6.1A, AD3)	0.97-1.66 μm (1)
Spectral Sampling ΔS		
- Prism 1 (Y-J)	100.0 >30 per pixel (TS6.1B, AD3, and TLR_C.4, AD1)	107.1
- Prism 2 (Y-H)	63.1	67.3

2.2 IFS Transmission

The IFS optical transmission was measured by comparing the flux measured using a Germanium sensor head (UDT Model 261) on the focal plane of the IFS, with that measured with the same sensor when located just in front of the BIGRE. The experiment was done using both Y-J and Y-H prisms (that is including filters and the masks on the intermediate pupil).
The sensor is sensitive over the wavelength range 0.8-1.7 μm; the detector has a square surface area of 0.5 cm^2. To ensure that this sensitive area is enough to cover the whole optical beam, a diaphragm with a diameter of 1.8 mm was inserted into the collimated beam provided by the CPS in front of the sensor (see Figure 4). An appropriate correction factor of ~1.006-1.018 (depending on wavelength) was included to account for the fraction of light lost when using the sensor because of its limited size. This correction depends on wavelength in relation to the part of the diffraction pattern generated by the diaphragm which falls within the sensitive area of the Germanium sensor head.

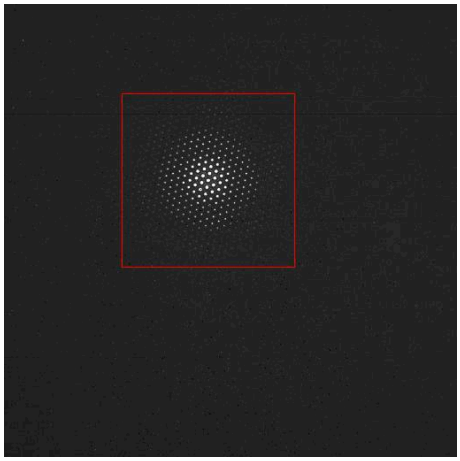

Figure 4. UDT 261 sensitive area (red square) compared with the image on the IFS focal plane obtained with the same optical configuration

To reduce the impact of the variation of the lamp fluxes and the drift of the detector zero level, the latter was frequently measured, and the whole experiment was repeated twice. Each time, five series of complete measurements: BEFORE-AFTER-BEFORE-AFTER-BEFORE have been taken. Results are shown in Figure 5 after the correction for the following two factors:

- Light falling out of the detector. As previously mentioned, we estimated a correction factor equal to ~1.006-1.018, depending on wavelength
- The losses due to the optics not included in the experiment, the dewar window, and the low pass band (LPB) filter. According to the data sheets, transmission of the dewar window is 0.987. The LPB filter transmission over the wavelength range 0.95-1.65 µm is 0.975 (measured by the vendor).

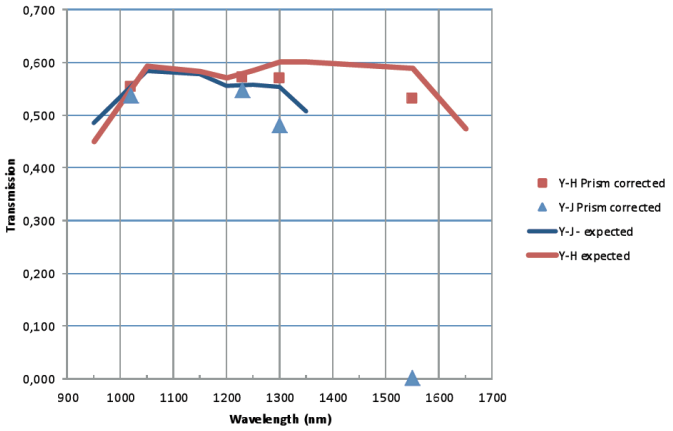

Figure 5. Corrected IFS transmission as a function of wavelength. Overimposed lines are expectations based on the transmission expected for the individual elements.

The average transmission value depends on the weight given to the values obtained at each wavelength. The approach we used started from the expectations (average values of 0.555 for the z-J mode, and 0.572 for the z-J-H mode, using trapezoidal integration). We corrected these values for the ratio between corrected and expected transmissions, interpolating (or extrapolating) linearly in wavelength. In this way, we obtain average transmission of 0.526 for the Y-J mode and 0.546 of the Y-H mode.

2.3 IFS Background

The instrument (thermal) background of the IFS has been measured acquiring images with the IFS sealed. The main source of background is thermal emission from the IFS, which is seen by the detector, with very minor contributions from dark current (~0.003 e-/s/pixel) and thermal emission from inside the dewar (<<1 e-/s/pixel). Most of the unwanted radiation is eliminated by the presence of a cold filter, about 40 mm in front of the detector; and by two baffles, a cold absorbing baffle located inside the dewar, and a warm reflecting baffle located on the back of the IFS camera. The purposes of the baffles are to have the detector only seeing cold components, as far as possible and reducing as much as possible reflection of radiation, which might cross the cold filter at large incidence angles. The residual thermal background is mainly due to unavoidable thermal emission from the active IFS optical components. This is temperature dependent. Hence, an important parameter to be checked is the bench temperature. The tests were then repeated at various bench temperatures. The expected thermal background was 23 photons/s/pixel for an ambient temperature of 285 K (=12 Celsius). We will assume this as the reference value.

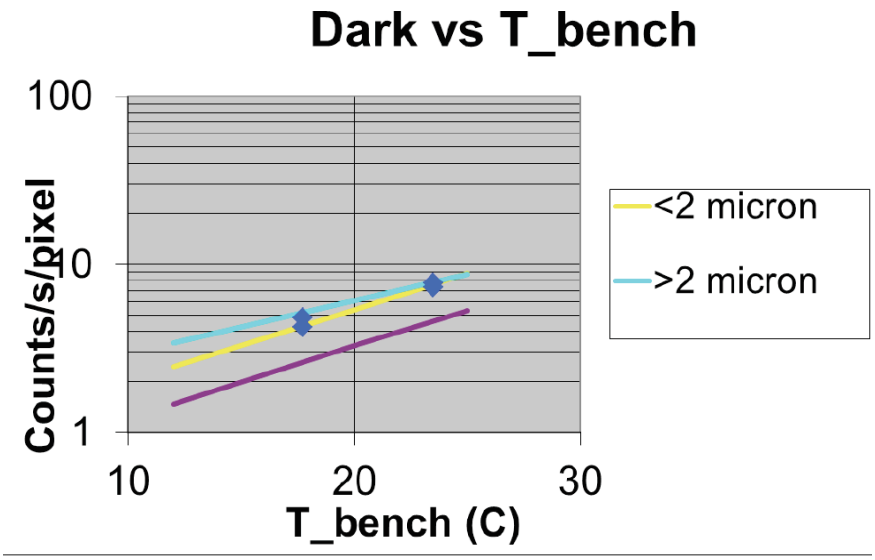

Figure 6: Run of IFS background as a function of temperature (blue symbols). Overimposed are the expected runs for those cases where background is dominated by short wavelength photons (<2 μm: yellow curve; this curve is indistinguishable from the predictions of our model for the thermal background) or long wavelength ones (>2 μm: cyan curve). The lower (violet) line represents expectations for the case where only photons emitted from the active surface of the last camera lens are considered.

In Figure 6, we plotted the measured values (blue diamond symbols), as well as three curves which represent:

- The run expected if the thermal background were due to short wavelength photons only (yellow line). The slope of this run is obtained by integrating the Planck function for the appropriate temperature with the cold filter transmission curve at incidence close to normal, as expected if the thermal background is due to light directly incident on the filter, without reflections within the cold baffle. The intercept was obtained by fitting the two data at the highest temperature.
- The run expected if the thermal background is due to long wavelength photons only (cyan line). The slope of this run is obtained by integrating the Planck function for the appropriate temperature with the cold filter transmission curve at large incidence angles with respect to normal, as expected in case

multiple reflections within the cold baffle dominates. The intercept was obtained by fitting the two data at the highest temperature

- The run expected if only photons emitted by the active surface of the last camera lens are considered (with an emissivity equal to 1). This last curve represents the absolute minimum thermal background that might be obtained by a perfect thermal design of the IFS.

Measured data are about 1.5 times the theoretical absolute minimum. To explain this difference, we constructed a model of the thermal background which takes into account the emissivity from the various surfaces seen by the detector (IFS camera, cold and warm baffle, dewar inner surface), multiple reflections on the cold baffle, cold filter and detector holder, as well as the transmission of the cold filter as a function of the angle of the incident radiation (using data provided by vendor). This model was successfully used in the optimization of the baffle system, which leads to the improvement in performances. According to this model, the most significant source of background is thermal emission seen through the IFS camera, which as mentioned above cannot be eliminated. This is followed by the warm filter, which is expected to contribute almost a fourth of the total. A minor contribution (about 10% of the total) comes from multiple reflections within the cold baffle. In principle, it should be possible to further reduce the warm baffle contribution by using a gold coating (emissivity of 0.025) rather than Al coating (emissivity of 0.09); in this way we might further gain a factor of about 1.2 in the thermal background. There was unluckily some technical problem in doing so. However, even as it is now, thermal background is very good. Using our model, which fits very well data and is virtually indistinguishable from the yellow curve of Figure 6, we can extrapolate the value at 12 C**.** We get a value of 2.5 counts/s/pixel, corresponding to 4.5 photons/s/pixel. This value is over a factor of 5 smaller than the value considered fiducial.

2.4 Laboratory Simulation of high contrast observation

We checked the high contrast properties of the instrument exploiting the good optical quality of the CPS (WFE<40 nm). The star has been simulated inserting a diaphragm (D= 0.2 mm) in the collimated beam of the CP. The diaphragm generated on the BIGRE a series of diffraction rings and the value of λ/D is ~4.9 lenslets at 1270 nm. Because the Strehl ratio was very high (0.987 @ 950 nm) we expect that the PSF is ~$3x10^{-4}$ of its peak value at ~30 lenslets from center (which would correspond to 0.37 arcsec when IFS is used with SPHERE at VLT). The source provides a maximum rate of about 4000 cts/s/pixel on the detector roughly corresponding to a non-coronagraphic observation of a star of magnitude J~9.5 (see Figure 7 for IFS in Y-H mode).

We acquired 50 images of 1 sec (total exposure of 50 sec). Data were reduced using the SPHERE data reduction and handling (DRH) recipes, and then visualized using the ATV command in IDL.

Figure 8 shows the results of data reduction. The DRH recipes rotate the images (by the angle between the BIGRE and the detector), and include the really observed area within a wider square frame. Note that the pinhole was not exactly centered on the BIGRE.

Diffraction rings (up to 5^{th} order) can be seen in the monochromatic median image. The good cosmetic of this median image allows visualizing well faint features. First, due to the electric cross talk between the different preamplifier outputs of the Hawaii II detector there are a number of "ghosts" of the central image. They have intensity of the order of slightly less than 1% of the central image, and may be both positive and negative. A strategy to eliminate these ghosts is under study. A second feature is the hexagonal structure due to coherent cross talk that is visible at a few counts level (that is ~10^{-3} of the central peak).

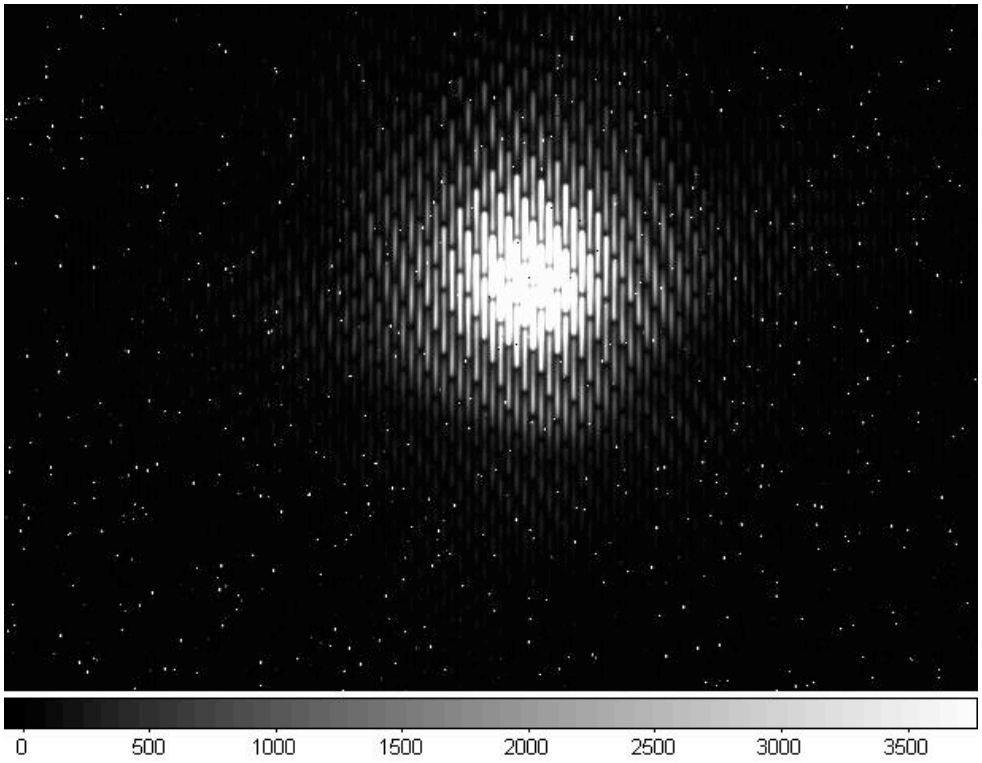

Figure 7. Portion of an image obtained by illuminating the BIGRE with a diaphragm inserted in the CPS (see Section 2). The IFS is in the Y-H mode. The image shown is the median of 50x1 sec observations.

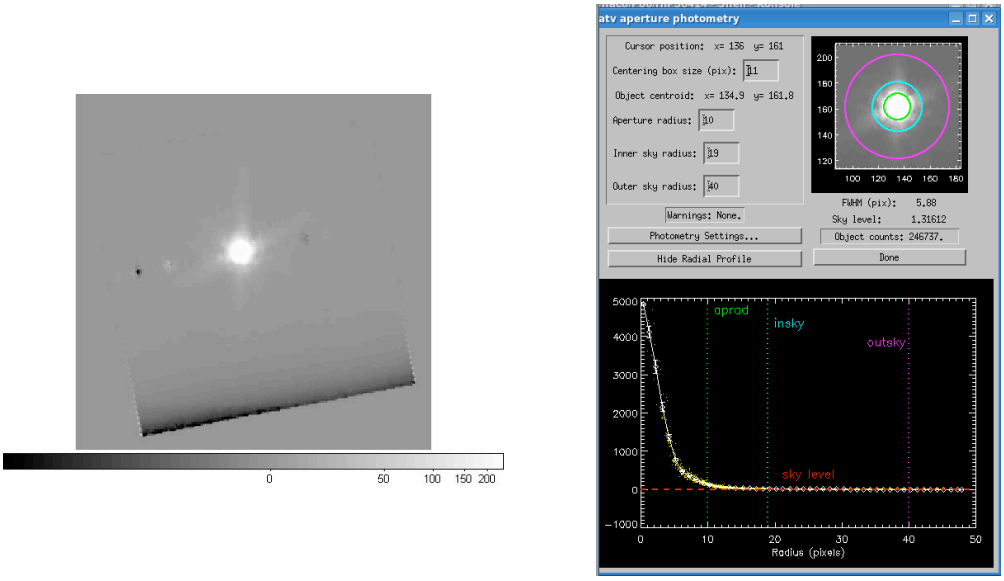

Figure 8. Left: median of the 39 monochromatic images. These images simulate a non-coronagraphic observation of a J=9.5 star obtained with IFS. The grey scale is logarithmic. Right: the PSF of the image obtained using ATV (an IDL routine)

The right panel of Figure 8 shows the PSF for the images of the left panel of Figure 8. The background level has been measured from the annulus between 19 and 40 pixels. In our simulation, this corresponds to the area between 0.23 and 0.49 arcsec from the star. In this area, the image has an average value of 1.32 counts, while the central peak is at 4900 counts. This yields a contrast of 2.7×10^{-4}.

We notice that the annulus between 19 and 40 pixels corresponds to an area in the range from ~4 to ~8 λ/D because in our simulated set up λ/D of the diffraction pattern provided by the diaphragm is about 5 pixels. The average contrast of the images produced by IFS for this area is very similar to what is expected for the Airy pattern generated by the diaphragm, which is the input illumination of the IFS. This implies that the calibration and analysis procedures allowed to retrieve the original illumination of the entrance at a reasonably good fidelity level.

While this observation is read out noise dominated over most of the field, and only a limited gain is then expected from application of differential imaging approaches, we run our own code for Speckle subtraction on this image. We then cross correlated the spectra of the datacube with that of a T7-star, simulating the search for an extrasolar planet. The result is shown in Figure 9 (left). The 5-σ contrast of this simulated observation is 1.2×10^{-4}.

Eventually, a deeper image was obtained with respect to that presented exploiting the same set up but with a number of DITs that has been raised from 50 to 320. The image was also dithered 4x4 using the appropriate instrument software (INS) template (the image actually consists of two 4x4 dithering sequences, with 10x1 s DITs in each dithering position). The new image reaches a 5-σ contrast of 5×10^{-5} (see Figure 9 right), which is the value expected. The contrast is limited by read-out noise.

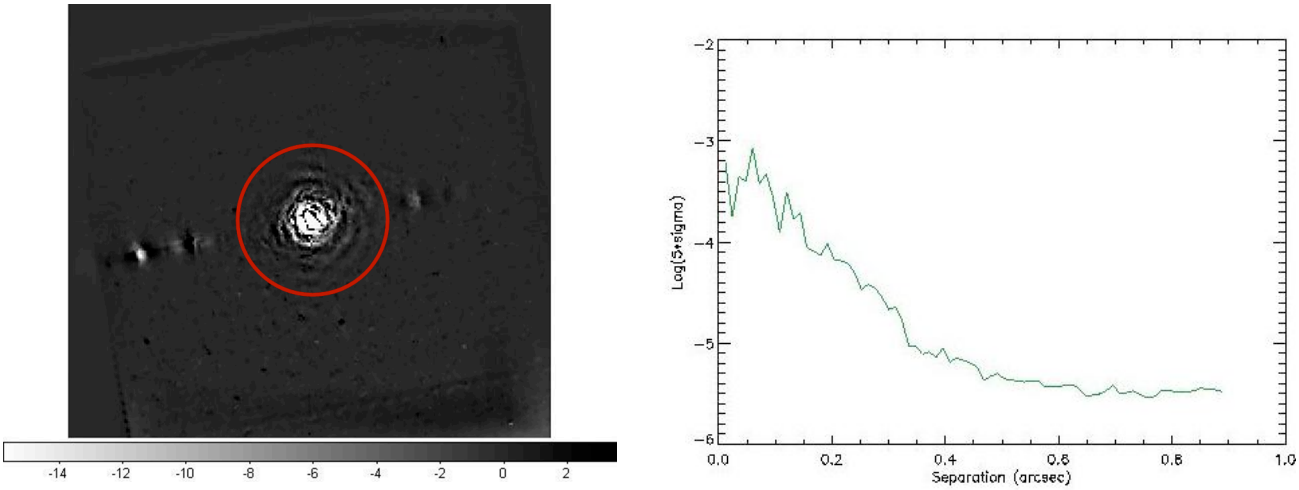

Figure 9. Left: Result of the application of the speckle subtraction technique. The grey scale is in counts, the peak value for the star being ~4100 counts. Right: Same as left panel but with a greater number of DITs (see text)

3. IFS INTEGRATION ON SPHERE

In December of the last year, IFS was moved from Padova to Grenoble IPAG where it was integrated together with IRDIS and ZIMPOL, on the SPHERE huge optical bench. After three different shift the Integral field spectrograph was mounted and aligned and all functionalities have been checked. In the next future we'll have several shifts in order to perform performance tests of IFS together with the whole SPHERE facilities.

Figure 10: IFS mounted on the SPHERE huge bench. Close up is the IFS Dewar.

4. CONCLUSION

The results of the tests described in this paper demonstrate the capability of the SPHERE-IFS instrument to fulfill all the requirements. The final instrumental test that will be performed in Grenoble by the summer of 2012, should allow to obtain a luminosity contrast of the order of 10^{-6} to 10^{-7} well fitted to perform imaging of giant extrasolar planets.

REFERENCES

[1] Wildi, F., Beuzit, J.-L., Feldt, M., et al., "SPHERE: the VLT planet imager in the post FDR phase", Proc. SPIE,7440, 21 (2009)

[2] Claudi, R.U., Turatto, M., Giro, E., et al., "SPHERE IFS: the spectro differential imager of the VLT for exoplanets search", Proc. SPIE, 7735, 30 (2010)

[3] Antichi, J., Dohlen, K., Gratton, R., et al., "BIGRE: A Low Cross-Talk Integral Field Unit Tailored for Extrasolar Planets Imaging Spectroscopy", ApJ, 695, 1042 (2009)